

# Models of optical/UV continuum in AGN. Constraints from NGC 5548 monitoring campaign.

Z. Loska<sup>1</sup> and B. Czerny<sup>1</sup>,

<sup>1</sup> Nicolaus Copernicus Astronomical Center, Bartycka 18, 00–716 Warsaw, Poland

## ABSTRACT

We analyse the data from the optical/IUE observational campaign of the Seyfert galaxy NGC 5548 in the context of 10 phenomenological models. On the basis of the optical/UV data as well as constraints from the X-ray observations we can favour one model of the nucleus: an accretion disc with an inner radius cutoff surrounded by a hot corona. The second acceptable model for optical/UV data is a distribution of optically thin clouds. However, X-ray constraints which were crucial in the analysis of disc type models could not have been applied; further development of this model is necessary.

**Key words:** accretion, accretion discs – galaxies: active – galaxies: Seyfert – X-rays: galaxies

## 1 INTRODUCTION

The nearby spiral galaxy NGC 5548 ( $z = 0.0174$ ) is one of the best laboratories for testing AGN models (Rokaki, Collin-Souffrin & Magnan 1993). The nucleus is bright (absolute visual magnitude -24.3), the interstellar extinction in this direction is exceptionally low (hydrogen column  $N_H \sim 1.65 \times 10^{20}$ , Nandra et al. 1991) and the nucleus is strongly variable in optical, UV and X-ray band. Extensive monitoring of that galaxy is reported in a number of papers devoted to optical (Peterson et al. 1991, Peterson et al. 1992, Peterson et al. 1994) UV (Clavel et al. 1991), and simultaneous Ginga & IUE campaign (Clavel et al. 1992). It was also one of the few AGN detected in usually unobserved EUV band (Marshall, Fruscione & Carone 1995).

The overall IR-UV spectrum (e.g. Ward et al. 1987) and X-ray spectrum (e.g. Nandra & Pounds 1994, Done et al. 1995) of the nucleus of NGC 5548 is fairly typical for a Seyfert 1 galaxy although the spectroscopic classification identifies it usually as Seyfert 1.5.

The amplitude of the variability of NGC 5548 is considerable at every wavelength from optical to hard X-rays.

In the optical band significant fraction of the luminosity is thought to be due to the contribution of starlight (e.g. Kotilainen & Ward 1994). The flux measured at 5100 Å varied by a factor 2 during the four years of the campaign (1988–1992). UV flux monitored in 1988–1989 varied almost by a factor 3 at 1350 Å.

As the continuum variations in all three UV bands and the optical band were simultaneous (down to a measurable delay of a few days; Clavel et al. 1991), most of the optical/UV variability can be accounted for by the reprocessing of hard X-rays, as suggested by Malkan (1991) and Collin-Souffrin (1991) (see also Krolik et al. 1991, Clavel et al. 1992, Rokaki et al. 1993). A dominant role for reprocessing is also consistent with Ginga data (Nandra & Pounds 1994)

which clearly show the presence of the reflection component superimposed on a typical hard X-ray power law (energy index  $\sim 0.9$ ), with reflected fraction of order the usual  $2\pi$ . Recent ASCA data (Mushotzky et al. 1995) support this conclusion as they show the  $K\alpha$  line profile consistent with a disc around a Kerr black hole inclined  $\sim 15^\circ - 38^\circ$  with respect to an observer. As the iron line is broad (FWHM  $> 35\,000$  km/s) most of the emission comes from the region smaller than  $\sim 36$  Schwarzschild radii. In most epochs the X-ray flux above 2 keV is strongly variable (factor 2 between separate observations, Nandra & Pounds 1994) but without systematic trends in the change of the energy index. In soft X-rays the variability pattern is more complex due to the presence of soft X-ray excess and the warm absorber (see Nandra et al. 1993 and Done et al. 1995 for ROSAT observations).

However, occasionally strong enhancements of the big bump component are seen (in UV in May 1984, Clavel et al. 1992; in soft X-rays in December 1992/January 1993, Done et al. 1995) which are unrelated to hard X-ray luminosity and indicate direct liberation of gravitational energy in the form of optically thick emission in these periods.

Multiwavelength studies put constraints on any models of the nucleus by determining or limiting the connections and delays between spectral bands. As for the continuum, both optical and UV spectra follow X-ray flux (with exceptions mentioned above) with the delay less than 6 days (Clavel et al. 1992). In the case of UV this delay is most probably smaller than 2 days which suggests the size of the UV emitting region of order of  $5 \times 10^{15}$  cm. Large amplitude changes in soft X-ray emission happen in 2 days and large amplitude variations of hard X-rays also require time scales of order of two days (e.g. Done et al. 1995).

The available data was mostly used to study the structure of the Broad Line Region (e.g. Done & Krolik 1996) as in that case the delays are well measurable.

A model of the continuum emission of NGC 5548 was elaborated by Rokaki et al. (1993). The model consisted of an inner disc emitting X-rays (modelled as a sphere of a constant radius and variable luminosity), an outer standard disc and an optically thin surrounding medium. The outer disc was irradiated by X-rays either directly or by photons scattered by the thin medium. Such a model adequately represented the data from IUE campaign but formal fits were not presented so a quantitative analysis was impossible.

In this paper we discuss a number of simple phenomenological models and we fit them to the data from the same observational campaign. We show that for the mass of the black hole  $6 \times 10^7 M_\odot$  (as estimated on the basis of X-ray reprocessing, UV and X-ray variability and emission lines) only two of these models are actually acceptable if the optical/UV data requirements are supplemented by the constraints from (non-simultaneous) X-ray data. The first of these two models is a non-stationary accretion disc with variable accretion rate and a variable inner radius cut-off. The gravitational energy available below the cut-off radius is liberated in the form of X-rays in the hot corona surrounding the disc and thermalized within the disc. The second model is the distribution of the (identical) optically thin clouds which emission in the optical/UV band can be approximated as a free-free emission.

The content of the paper is following. Models are described in Section 2. In Section 3 we describe the method of analysis of the data including the problem of the starlight contribution and the contribution of Balmer continuum and blended FeII lines at 2670 Å. The results are given in Section 4. Section 5 contains the discussion of the results. Conclusions are given in Section 6.

## 2 MODELS OF OPTICAL/UV CONTINUUM

We introduce a number of viable models describing the extension of the optically thick disc-like part of the flow and the geometry of the source of X-ray radiation. As there are no detailed theoretical predictions about the formation of these two phases of accreting gas we introduce phenomenological parameters but with a physically sound interpretation. All models considered here do not contain more than two free time-dependent parameters as we fit only a time sequence of four frequency points. However, models may contain additional parameters not varying with time, like the mass of the central black hole etc., as they do not reduce noticeably the number of the degrees of freedom.

The first three models are based on the assumption that the only variable component is the X-ray flux incident upon a stationary accretion disc. The next five models are based on variations in the accretion rate at the innermost part of the disc which in turn may cause a change in irradiation. As a single optical/UV spectrum consists of only 4 points we approximate the local thermal emission of the disc by a black body with the effective temperature distribution calculated including the viscous dissipation (determined by accretion rate) and the irradiation flux appropriate for adopted geometry (taking albedo equal 0.9). We assume non-rotating black hole, i.e. Schwarzschild geometry.

The next model is the simplest version of emission by optically thin clouds. Finally, we also fit a single power law model for a better discussion of the quality of the data.

### 2.1 Stationary accretion disc and a point-like X-ray source

This model consists of a standard stationary Keplerian disc around a massive black hole of the mass  $M$  and accretion rate  $\dot{M}$ , and a point-like source of X-ray radiation localized on the disc symmetry axis and characterized by the luminosity  $L_X$  and distance from the disc plane  $H_X$ . Such a geometry was frequently suggested and it was used in a number of papers devoted to modelling AGN emission (e.g. Ross & Fabian 1993, Życki & Czerny 1994). It may for example approximate the situation where hard X-ray emission is produced by shocks which may accompany the formation of the jet (e.g. Henri & Pelletier 1991, Liang & Li 1995). Since it was suggested that the variable irradiation is mostly responsible for the variable optical/UV emission (Clavel et al. 1991, Rokaki et al. 1993) we assume that  $\dot{M}$  is constant whilst  $L_X$  and  $H_X$  vary. The local effective temperature in the disc is calculated by taking into account the stationary viscous flux and the thermalized X-ray flux. Computing the last term we assume that the albedo for X-rays is equal 0.9 as determined by Lightman & White (1988) (see also Życki et al. 1994) as the reflection component observed in hard X-ray data indicates the presence of neutral gas (Nandra et al. 1991).

### 2.2 Stationary accretion disc with geometrically thick optically thin inner part

As the standard accretion disc model with  $\alpha P$  viscosity (Shakura & Sunyaev 1973) is thermally unstable in the inner parts the inner disc may become optically thin and hot. Such a flow was studied in a number of papers (Shapiro, Lightman & Eardley 1976, Wandel & Liang 1991, Kusunose & Zdziarski 1994). The physics behind this is complex but a simplified geometrical model can be used: the transition radius  $R_X$  defines the cut-off radius for the optically thick standard disc (e.g. Siemiginowska & Czerny 1989). The inner part of the disc is replaced with inner optically thin disc of the luminosity  $L_X$ . The shape of the inner disc is approximated by a sphere of a radius  $R_X$ . We do not require that the gravitational energy available below  $R_X$  is equal to  $L_X$  in order to account for possible magnetic storing of the energy in the optically thin region. The sphere irradiates the outer optically thick parts of the disc. A similar model was actually fitted to the light curve of NGC 5548 by Rokaki et al. (1993). The difference between their model and the one presented here is in their assumption of constant  $R_X$  ( $3 \times 10^{14}$  cm) and the presence of additional irradiation of the disc due to an extended hot medium. In our model we assume a constant accretion rate in the outer parts of the disc but allow for variations of both  $L_X$  and  $R_X$ . It again implies some storage of the energy by the inner disc.

### 2.3 Stationary accretion disc irradiated by a hot corona

A number of papers were devoted to the scenario in which most of the energy is dissipated in the disc corona instead of the disc interior (e.g. Liang & Price 1977, Paczyński 1978; Życki, Collin-Souffrin & Czerny 1995). We roughly model such a situation assuming that standard stationary

accretion disc of a given  $M$  and  $\dot{M}$  is irradiated by the corona effectively producing the local flux

$$F_{cor} = A(r/3r_g)^{-\beta} \quad (1)$$

where both  $A$  and the index  $\beta$  were allowed to vary. To express the model parameters more conveniently we use the bolometric luminosity of the corona rather than the coefficient  $A$  (both are easily related by the integration over radius, i.e.  $L_X = 18\pi A r_g^2 / [(r_{out}/3r_g)^{2-\beta} - 1] / (2 - \beta)$  for  $\beta$  different from 2). In this model the strength of the corona is unrelated to the accretion rate.

#### 2.4 Non-stationary accretion disc with advection-dominated innermost part

The timescale of the UV variability of order of a few days is actually consistent with the viscous timescales of the inner few Schwarzschild radii if the viscosity parameter is high (see e.g. Siemiginowska & Czerny 1989). Therefore we study the hypothesis that the observed spectral changes are actually driven by the variations in the accretion rate. In this model we assume that the innermost part of the disc may become optically thin. If such optically thin flow is dominated by advection (e.g. Narayan & Yi 1995) only a small fraction of energy released in this part of the flow would emerge in the form of X-rays and irradiate the optically thick parts. Since this X-ray emission can then be an arbitrarily low fraction of the available gravitational energy we neglect the irradiation as the data is not good enough to introduce another free parameter.

Therefore in this model we simply assume that the standard disc extends down to a certain cut-off radius  $R_C$  and the part of the disc below does not contribute to UV radiation flux.

#### 2.5 Non-stationary accretion disc with inner radius cut-off and a point-like X-ray source

If the gravitational energy cannot be stored efficiently by the magnetic field the model 2.1 of the point-like source is incorrect. Therefore we consider another model in which an accretion disc extends only down to a certain cut-off radius  $R_C$ . The remaining available energy not dissipated in the disc is now dissipated in the point-like source. Such a model is motivated for example by suggested ejection of plasmoids at the expense of the gravitational energy of the inner part of the disc (e.g. Liang & Li 1995). We assume that the X-ray source is located on the symmetry axis at the distance  $R_C$ . We allow now for variable accretion rate in the disc  $\dot{M}$  as the cut-off radius may (in fact, should) depend on it. Therefore the model again has two variable parameters.

#### 2.6 Non-stationary accretion disc with geometrically thick optically thin inner part

If the energy cannot be stored efficiently by the inner hot part of the disc as it can in model 2.2 the luminosity of this part has to be matched by the available gravitational energy below  $R_X$ . In close analogy with model 2.2 we now choose the disc accretion rate  $\dot{M}$  and the cut-off radius  $R_X$  filled by the spherical inner disc as our variable parameters; the bolometric luminosity of the sphere and the effect of irradiation

of the disc by its X-ray emission are uniquely determined by these two values. The model is also complementary to model 2.4 as this time we neglect the advection losses and we allow for the irradiation of the optically thick parts of the disc.

#### 2.7 Non-stationary accretion disc with inner radius cut-off and scattered X-ray radiation

This model differs with respect to the previous two in the geometry of the irradiation by X-ray. This time we assume that the luminosity is released in the center and redirected towards the disc by scattering in an optically thin hot medium. Effectively, we just make the assumption that the incident luminosity is inversely proportional to the square of a distance. Similar dependence on a distance was adopted in the next model but this time the cut-off radius enters the luminosity only through the total X-ray luminosity whilst in the corona model 2.8 the cut-off radius would enter also through the normalization.

#### 2.8 Non-stationary accretion disc with inner radius cut-off irradiated by the corona

This model differs from the model 2.3 as now we consider the specific example of the dependence of the corona parameter on the accretion rate in the disc. We now assume that the standard disc extends not to the marginally stable orbit but only to a certain cut-off radius  $R_C$  as in model 2.4. The gravitational energy below this radius is now exchanged into X-ray photons and redirected towards the disc by the corona or dissipated by the corona according to the law

$$F_{cor} = A(r/R_C)^{-\beta} \quad (2)$$

where  $A$  is determined by the available bolometric luminosity below  $R_C$ . As fits of the model 2.3 (see Figure 3) to the data favoured the value  $\beta$  about 2, we fixed  $\beta$  in the present model mostly at the value 2. Therefore our model has again only two independent parameters.

#### 2.9 Free-free emitting clouds

As the existence of accretion discs in the centers of active nuclei is questioned (see e.g. Barvainis 1993) and optically thick clouds (e.g. Guilbert & Rees 1988, Lightman & White 1988, Sivron & Tsuruta 1993) or optically thin clouds (Antonucci & Barvainis 1988, Ferland, Korista & Peterson 1990) reprocessing hard X-ray radiation are suggested to be responsible for emission in the optical/UV/soft X-ray band we consider a cloud model as well. We assume that clouds are optically thin for absorption (nevertheless they can be optically thick for scattering) and their radiation can be well approximated as a bremsstrahlung emission at a single temperature  $T$ . Such a spectrum has two parameters: the temperature  $T$  and normalization  $V$

$$F_\nu = V g_{ff}(\nu, T) T^{-1/2} \exp(-h\nu/kT) \quad (3)$$

where the Gaunt factor  $g_{ff}(\nu, T)$  is taken from Gronenschild & Mewe (1978). The normalization  $V$  is proportional to the emitting volume and to the square of the electron density.

We introduce this model due to its recent popularity but it is necessary to realize that real cloud spectra would be dominated by strong emission lines, particularly for temperatures lower than  $\sim 10^6$  K (e.g. Krolik & Kriss 1995, Collin-Souffrin et al. 1996).

## 2.10 Power law model

In order to check how important is the correct determination of the spectrum curvature in the successful models we also fit a simple power law to the same data, with the slope and the normalization being free-parameters of this formal model. Such a pure power law model has no direct physical interpretation although a contribution of a power law component to the optical data of unspecified origin has been broadly discussed (e.g. Loska & Czerny 1990). Also, in the course of analysis of the BLR contribution to the continuum an assumption was made that the continuum can be approximated as a power law so the fit serves as a test of this hypothesis.

## 3 METHOD OF ANALYSIS

### 3.1 Observational data

#### 3.1.1 Observational campaign

As the contribution of starlight might be considerable in the optical band and its influence strongly decreases with the studied frequency we concentrated on the analysis of the continuum when the UV data are available. The IUE observations of NGC 5548 covered the period December 1988 – August 1989 and the fluxes at 1350Å, 1840Å, 2670Å (SIPS) were taken from Clavel et al. (1991), and 5100 Å from Peterson et al. (1992). We favoured the 5100 Å value over the 4870 Å flux from Peterson et al. (1991) as the second quantity is contaminated by the  $H_\beta$  emission and therefore less accurate, as argued by Peterson et al. (1992). The optical measurements were carefully corrected by observers for the aperture effects and reduced to a standard (A) set taken with the aperture  $5.0'' \times 7.5''$ .

#### 3.1.2 Starlight problem

The flux measured at 5100 Å is thought to be contaminated by starlight from the host galaxy. The original optical data measured using different instruments and apertures was corrected in such a way that only the starlight present in the small aperture data  $5.0'' \times 7.5''$  remained. As the method did not rely on any specific spectral shape of the starlight the adopted procedure was actually independent from the nature of the extended emission.

However, in order to model the intrinsic variability of the nucleus all the starlight contribution had to be removed from the data. For that purpose we assumed that the shape of the starlight in NGC 5548 was well represented by the emission from the nucleus of M31, as shown by Wamsteker et al (1990). We adopted the relative starlight contribution at 5100 Å in the standard aperture equal  $3.4 \times 10^{-15}$  erg/s/cm<sup>2</sup> after Romanishin et al. (1995). Having such normalization, we subtracted the starlight from all four frequency points although at 2670 Å and 1840 Å and clearly at 1350 Å its contribution is actually negligible (never higher than two per cent).

#### 3.1.3 Balmer continuum and blended FeII lines

The flux at 2670 Å is additionally contaminated by contribution from the BLR. Peterson et al (1991) estimate this

contribution as 20 % of the measured flux. However, the variations of the nuclear emission are followed by variations of the Balmer continuum and blended FeII emission with possibly smaller amplitude and a delay of order of a few days. Maoz et al. (1993) therefore made much more detailed analysis of the BLR continuum. They showed that the typical delay of the emission due to the blended Fe lines was of order of 10 days and they determined the total luminosity of this component in the band 2160 Å – 4130 Å in each data set. We therefore calculate the correction to the 2670 Å flux as a mean flux in this spectral band and we adopt 20% of this value as an error, as suggested by the authors. There may be a contribution of the BLR to the 1840 Å at a level up to 10 % but this effect is smaller than the correction at 2670 Å and not studied so carefully so we did not include it while correcting the data.

### 3.2 Fitting procedure

We fit the models to the data calculating the value of  $\chi^2$  at every time point separately, so

$$\chi^2 = \sum_{i=1}^4 \frac{(y_{obs}^i - y^i(a_1, a_2))^2}{\sigma_i^2} \quad (4)$$

where  $y_{obs}^i$  is the observed value and  $y^i(a_1, a_2)$  is calculated from any of our two-parameter model. Errors  $\sigma_i$  of the measurements at 1350 and 1840 Å are taken directly from the Table 2 (SIPS) of Clavel et al. (1991) while errors at 2670 Å were calculated assuming the errors of the subtracted BLR continuum equal to 20% of the determined flux and the error of subtracted starlight at 5100 Å was taken equal to the error of the total flux at minimum.

We search for the minimum with respect to the parameters  $a_1$  and  $a_2$  at every time point using the procedure AMOEBA from Numerical Recipes (Press et al. 1989). In order to accept or to reject the model we calculate the global value of the reduced  $\chi^2$  for a given model (i.e. we sum the contributions to  $\chi^2$  from all four frequencies in all time points and divide by the number of the degrees of freedom, including these connected with the global parameters) while the fits at every time point give us the value of the model parameters as functions of time.

## 4 RESULTS

### 4.1 Fits of theoretical models

The last two models, namely the free-free emission (model 2.9) and a power law (model 2.10) do not include any global model parameters apart from the two parameters varying with time so their analysis is the simplest.

The variations of the energy index with the luminosity clearly show the well known trend in Seyfert spectra, i.e. the spectrum is harder when the source is brighter. However, the curvature is the essential property of the spectrum so the fit of the model 2.10 to the data is poor (see Table 1). Any model giving the  $\chi^2/dof$  above  $\sim 1.52$  can be rejected at the 99.9% confidence level for the number of the degrees of freedom between 89 and 92 in presented models. It means that the approximation of the continuum with a power law used to analyse the BLR contribution is not very

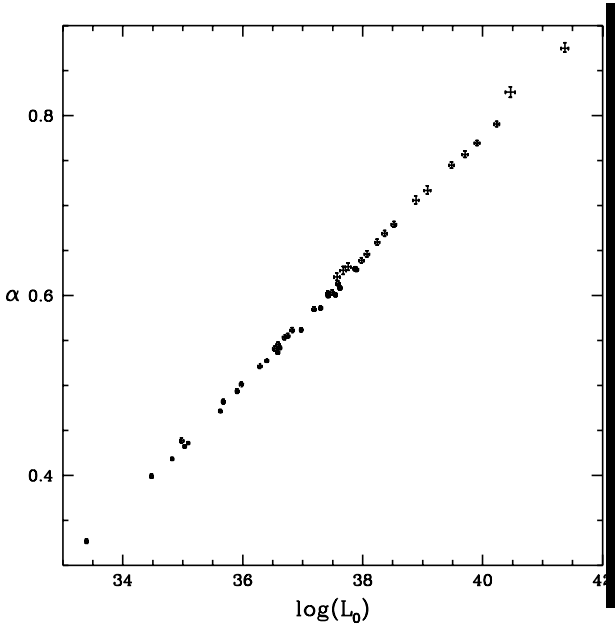


**Figure 1.** Energy index versus the normalization constant  $L_0$  for a power law fit (model 2.10). Error bars represent 90 % confidence level.

accurate. This may also mean that the continuum obtained by subtracting BLR contribution estimated on the basis of a power law shape of the continuum may also contain some systematic errors.

A better fit is provided by the free-free isothermal model. The variable temperature allows it to account for the variable spectral curvature. The total  $\chi^2$  is only marginally above 1 so the model is acceptable. The model contains a strong correlation between the temperature and the normalization factor. It means that either volume, or the density (or both) increase when the temperature increases although the relative change in temperature is more than a factor 2 larger. This trend is not in contradiction with the expected behaviour. If the timescale for expansion of the clouds under variable irradiation is long we expect no variations of the volume measure. If this timescale is short and the cloud adjusts itself to constant ionization parameter  $\Xi$  to preserve its thermal stability (e.g. Collin-Souffrin et al. 1996) the density may indeed decrease with an increase of irradiation giving in effect an increase in the measure of emission  $V$  as defined in the model (i.e. proportional to the product of the emitting volume and the square of the electron density). However, the presented result should not be treated as a satisfactory test of the cloud model since the temperatures appropriate for the overall curvature of the spectrum are not much higher than  $10^5$  K and the analytic free-free formula is not an adequate description of the spectrum actually dominated by line emission.

All the remaining models contain some global model parameters. We fix the value of the mass of the central black hole on the basis of available information. However, as the adopted value can be questioned, we show the major trends in the dependence on global parameters in Section 4.3. Other parameters ( $\beta$  in model 2.8 and  $\dot{m}$  in models 2.1, 2.2 and 2.3) are chosen arbitrarily but the dependence of the fits on these parameters were tested.

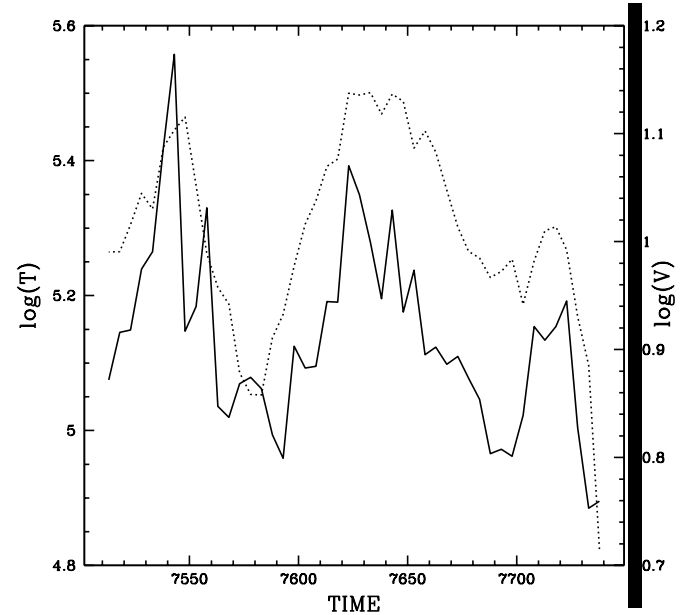


**Figure 2.** Temperature  $T$  (continuous line) and emission measure  $V$  (normalization constant proportional to the square of the electron density and the gas volume; dotted line) as functions of time for a free-free emission (model 2.9)

The mass of the central massive black hole seems to be known relatively well. Its value most probably lies between  $5 \times 10^7 M_\odot$  and  $6 \times 10^7 M_\odot$  (Rokaki et al. 1993), and X-ray observations confirm the inclination angle  $\sim 20^\circ - 30^\circ$  used to derive these limits.

X-ray reprocessing also supports this value directly. The delay of the UV emission with respect to the X-ray data not more than by two days indicate that the reprocessing region is of order of  $5 \times 10^{15}$  cm. The same region should be responsible for the formation of the broad  $K_\alpha$  Fe line. The width of the line larger than 35 000 km/s corresponds to the Keplerian orbit below  $\sim 36r_g$ . The two dimensions are in mutual agreement for the mass of the central black hole about  $6 \times 10^7 M_\odot$ .

Direct modelling of the optical/UV data with an accretion disc gave the upper limit for the value of the black hole  $5 \times 10^8 M_\odot$  (Loska et al. 1993). The estimates of the mass of the black hole based on the kinematics of the Broad Line Region lead to the value about  $10^8 M_\odot$  (e.g. Wanders et al. 1995) or somewhat smaller (Done & Krolik 1996).

Therefore in our basic analysis we adopt the value of the mass of the black hole of  $6 \times 10^7 M_\odot$ , obtained from the most accurate estimates and consistent with all available constraints.

For this value of the central black hole we found that only the models 2.3 and 2.7 do not fit the data. All other models well represent the behaviour of the optical/UV flux. Fits of model 2.3 with larger and smaller values of  $\dot{m}$  does not improve the fit considerably as the model only weakly depends on  $\dot{m}$ . Model 2.7 does not include additional global parameters, apart from the mass of the black hole.

This result is not surprising as all the models were designed in such way as to have enough of flexibility. However, the constraints on the model parameters lead to very interesting results.

**Table 1.** The values of  $\chi^2$  per one degree of freedom. Models are numbered according to the corresponding paragraphs. Adopted values of global parameters (mass of the black hole in solar masses and accretion rate in Eddington units or the index  $\beta$ ), if appropriate, are given in column 2 and 3.

Model	Mass/ $M_\odot$	$\dot{m}$	$\chi^2/\text{dof}$
2.1	$1 \times 10^7$	0.01	1.05
	"	0.1	0.87
	"	0.5	0.99
	$6 \times 10^7$	0.01	0.87
2.2	$1 \times 10^8$	0.005	0.93
	$5 \times 10^8$	0.001	0.67
	$1 \times 10^7$	0.01	1.03
	"	0.1	1.03
2.3	"	0.5	1.03
	$6 \times 10^7$	0.1	1.01
	$1 \times 10^8$	0.005	1.02
	$5 \times 10^8$	0.001	2.69
2.4	$1 \times 10^7$	0.01	2.66
	"	0.1	2.86
	"	0.5	4.22
	$6 \times 10^7$	0.001	2.16
2.5	"	0.005	2.22
	"	0.01	2.31
	$1 \times 10^8$	0.005	1.76
	$5 \times 10^8$	0.001	0.61
2.9	—	—	1.15
2.10	—	—	2.68
Model	Mass/ $M_\odot$	$\beta$	$\chi^2/\text{dof}$
2.4	$1 \times 10^7$	—	92.65
	$6 \times 10^7$	—	0.81
	$1 \times 10^8$	—	0.81
	$5 \times 10^8$	—	7.33
2.5	$1 \times 10^7$	—	5.78
	$6 \times 10^7$	—	0.93
	$1 \times 10^8$	—	0.87
	$5 \times 10^8$	—	7.33
2.6	$1 \times 10^7$	—	92.31
	$6 \times 10^7$	—	0.75
	$1 \times 10^8$	—	0.76
	$5 \times 10^8$	—	7.33
2.7	$1 \times 10^7$	—	5.35
	$6 \times 10^7$	—	2.65
	$1 \times 10^8$	—	1.54
	$5 \times 10^8$	—	7.33
2.8	$1 \times 10^7$	2.0	7.73
	$6 \times 10^7$	1.8	5.34
	"	2.0	0.94
	"	2.2	2.47
2.9	$1 \times 10^8$	1.8	0.55
	"	2.0	0.51
	"	2.2	0.48
	$5 \times 10^8$	2.0	7.33

Of the three stationary models, the first two are clearly acceptable which means that we cannot differentiate between the point-like X-ray source and an extended source of X-ray emission. However, it is interesting to note that in both cases involved X-ray luminosity is considerably larger

(factor 2 to 17) than the luminosity viscously liberated in a disc. It is generally not surprising as the variable irradiation has to account for the observed amplitude of the flux changes.

The second property the two models have in common is the relatively large height of the X-ray source above the disc plane; the radius of the optically thin sphere or the height of the point-like source above the disc plane is of order of 30 - 60  $r_g$ . Such a constraint was by no means imposed on the models.

Among the non-stationary models, only model 2.7 is not acceptable. The remaining models provide good fits to the data. Again, all of them show very similar behaviour. The variability is driven by the change in accretion rate (by a factor up to 3) around a value of order of 0.2. The cut-off radius vary less and in all cases it is anticorrelated with the accretion rate; the effect is the strongest in model 2.7 and almost invisible in model 2.4.

One of these models (model 2.4) does not include any irradiation by X-rays. The model fits the data well. For the value of the mass of the central black hole adopted in these calculations the cut-off radius is practically uncorrelated with the accretion rate. Nevertheless, its presence is the essential part of the model. Fits of the same model with the cut-off radius fixed at the mean value ( $\sim 16.5r_g$ ) are much worse ( $\chi^2 = 3.00/\text{dof}$ ). It might mean that the transition from the optically thin to optically thick solution in the innermost part of the disc is not determined by the accretion rate but by some other external parameter, e.g. magnetic field. Although not intuitive, such a possibility cannot be easily excluded.

If the irradiation is allowed the variations of accretion rate are of smaller amplitude than in the model 2.4 as they are enhanced by absorbed X-rays. Although in all models there is a weak anticorrelation of the cut-off radius and the accretion rate, the liberated X-ray luminosity is directly correlated with the accretion rate although the dependence is somewhat weaker than linear.

In these models the height or the size of the X-ray source is about a factor 2 smaller than in models with constant accretion rate so the match consistent with  $K_\alpha$  constraints is much easier to achieve.

The two models (2.3 and 2.7) are unable to fit the data as they do not produce enough of the spectrum curvature in the UV band. They well represent the NGC 5548 when it is bright but they are unable to model the spectrum when the object is fainter and the maximum of the spectrum is clearly seen on the  $\log(\nu f_\nu)$  vs.  $\log(\nu)$  diagram. However, this conclusion is changed if we allow for larger mass of the central black hole (see Sect. 4.3).

It is interesting to note that anomalously high continuum measurement at optical wavelength on JD 2,447,546 discussed by Peterson et al. (1991) is reproduced by models 2.3, 2.7, 2.8, 2.9 and 2.10 but not by the others.

#### 4.2 Constraints from the X-ray observations

There was no continuous coverage by any X-ray satellite during the IUE campaign analysed in detail in this paper. However, shorter simultaneous observations were carried out with Ginga satellite (Clavel et al. 1992). Also recent high quality ASCA observations put constraints on the models.

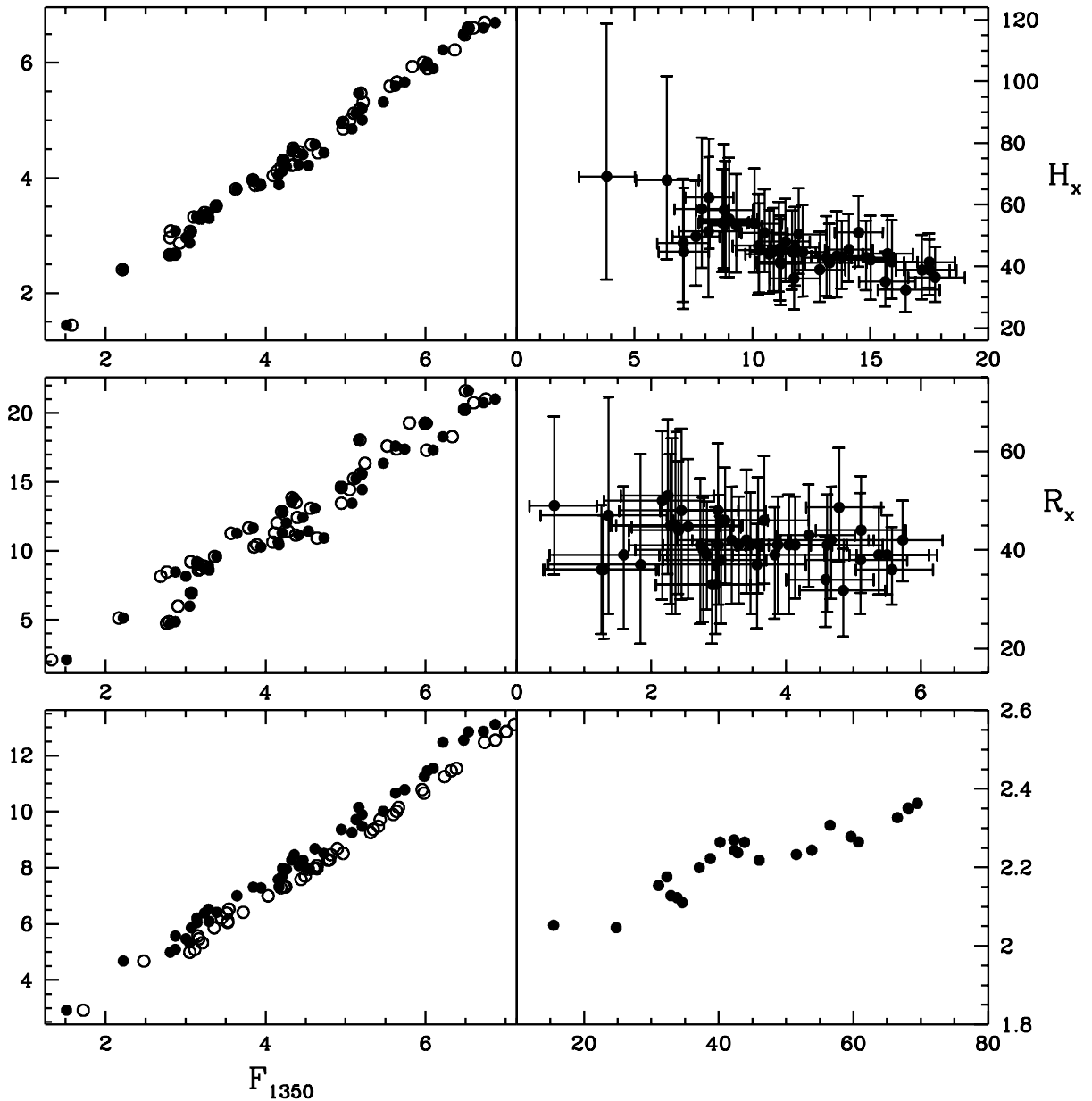


**Figure 3.** Stationary models: model 2.1 - upper panel, model 2.2 - medium panel and model 2.3 - lower panel. The left side of the diagram shows the dependence of the X-ray bolometric luminosity of the model  $L_X$  measured in  $10^{44}$  erg/s versus the flux at 1350 Å in units  $10^{-14}$  erg/s/cm<sup>2</sup>/Å as measured directly (full dots) and as derived from the best fit model (open circles). Right side of the diagram shows the dependence of the height of the point-like source  $H_X$  in  $r_g$  units, the size of the optically thin part of the disc  $R_X$  in  $r_g$  and index  $\beta$ , for models 2.1, 2.2, 2.3 correspondingly, as functions of the X-ray bolometric luminosity, this time measured in units of the accretion disc viscous luminosity. Error bars represent 90% confidence level.

These additional requirements can be used to reduce the number of models allowed by the optical/UV data alone.

The simplest constraint comes from the mean bolometric X-ray luminosity. Although its value is not known accurately due to the uncertainty of the high energy extension of the hard X-ray power law but a reasonable estimate gives value up to  $5.5 \times 10^{44}$  erg/s (Done et al. 1995) when the

source is bright (for an adopted value of the mass of the central black hole this luminosity translates into  $\dot{m} = 0.08$ ). During the campaign analysed in this paper the source was generally dimmer. All the models containing the irradiation should return an X-ray luminosity of order or below this limit. This condition is satisfied by models 2.1, 2.5 and 2.8 (among the models with acceptable  $\chi^2$ ) but not by models

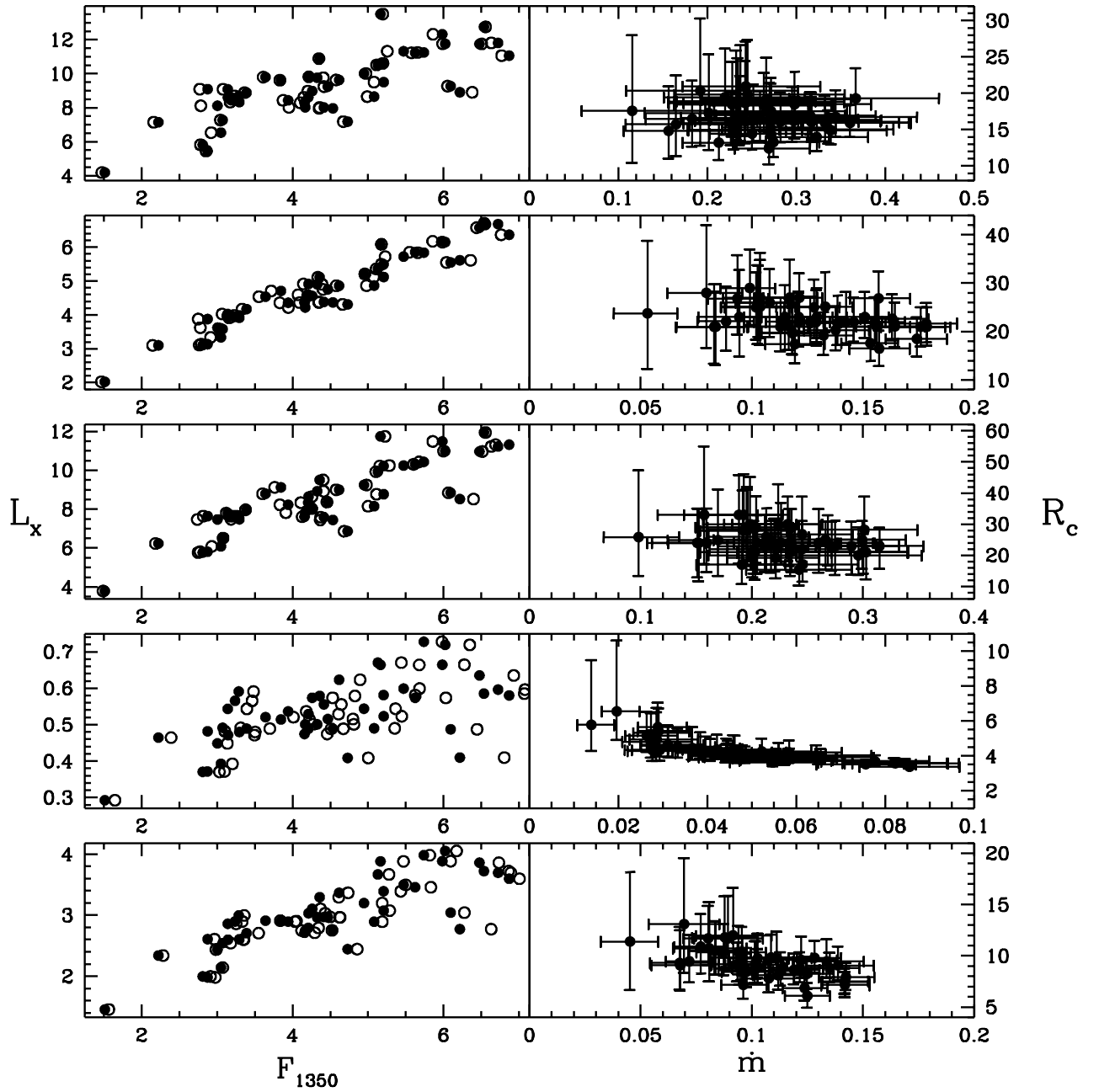


**Figure 4.** Non-stationary models: panels from the top to the bottom show models 2.4, 2.5, 2.6, 2.7 and 2.8. The left side of the diagram shows the dependence of the X-ray bolometric luminosity of the model  $L_X$  measured in  $10^{44}$  erg/s versus the flux at  $1350 \text{ \AA}$  in units  $10^{-14}$  erg/s/cm $^2/\text{\AA}$  as measured directly (full dots) and as derived from the best fit model (open circles). In the model 2.4 the X-ray energy shown is the total energy available below the cut-off radius; most of this energy is advected and only an arbitrarily low fraction of it might eventually emerge in the form of X-rays. Right side of the diagram shows the dependence of the cut-off radius of the disc  $R_C$  in  $r_g$  as function of the accretion rate measured in Eddington units. Error bars represent 90 % confidence level.

2.2 (for  $\dot{m} = 0.1$ ), and 2.6 (see Fig. 4 and Table 1). Allowing for lower  $\dot{m}$  in model 2.2 still increases the luminosity. Larger value of accretion rate leads to acceptable luminosities but at the same time it increases the cut-off radii to unacceptable values larger than  $36 r_g$  (see below).

The constraint does not apply to model 2.4 as in this case the energy flux available for X-ray production is mostly

advected below the horizon of the black hole.

The result of the X-ray monitoring was the proportionality of the X-ray luminosity and  $1350 \text{ \AA}$  flux, with flattening when the  $1350 \text{ \AA}$  flux was above  $5 \times 10^{-14}$  erg/s/cm $^2/\text{\AA}$ . Therefore in Fig. 3 and Fig. 4 we plot the X-ray luminosity derived from models versus  $1350 \text{ \AA}$  flux. We see that the scatter on the diagrams showing stationary models is

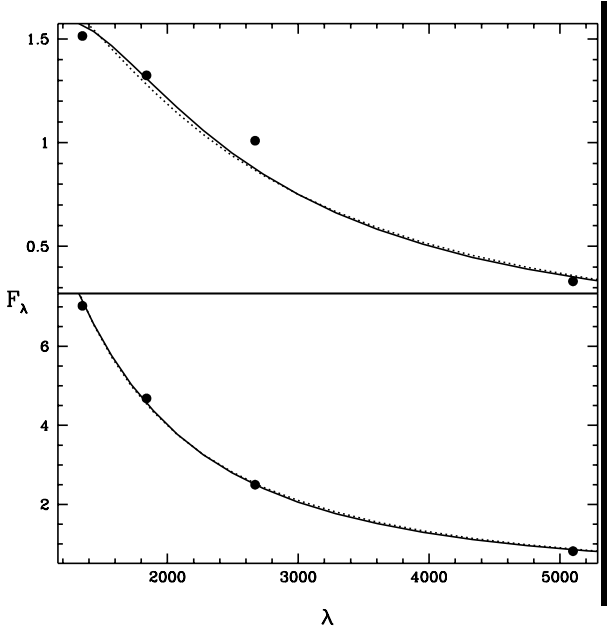


**Figure 5.** Observed optical/UV spectrum of the nucleus when the source was faint (date 7738 - upper panel) and when it was bright (date 7622 - lower panel) are shown with dots. Best fits to the data by the corona model 2.8 is marked as continuous line and the best fit of the free-free model 2.9 is marked with a dotted line.  $F_\lambda$  is given in units  $10^{-14}$  erg/s/cm $^2$ /Å and  $\lambda$  in Å.

much smaller than in the observational data in Fig. 4 of Clavel et al. (1992). We can also use the formula from Clavel et al. (1992) to predict the range of the 2-10 keV flux expected from the observed range of the 1350 Å flux. If we additionally use the bolometric correction of Done et al. (1995) we estimate the total X-ray luminosity range to be  $(1.4 - 5.1) \times 10^{44}$  erg/s. X-ray luminosities derived for the models 2.1, 2.5 and 2.8 cover just this range.

The strength of the observed  $K_\alpha$  line requires that approximately half of the X-ray flux is reprocessed by the disc and the other half reaches an observer without interaction with the disc. This requirement is approximately satisfied by all models in which irradiation is present as the optically thin part of the disc is never significantly larger than the height, or extension, of the X-ray source so almost half of the flux can be intercepted.

ASCA observations in turn constrain the geometry of the models. According to these data (Mushotzky et al. 1995) the  $K_\alpha$  iron line has the FWHM larger than 35 000 which corresponds to Keplerian orbits below  $\sim 36r_g$ . It has two consequences.

The first limit imposed on the models is that the optically thick part of the disc extends considerably below  $36r_g$ . This condition is satisfied by models 2.1, 2.4, 2.5 and 2.8 as well as by some other models rejected on the grounds of their high X-ray luminosity.

The requirement that most of the line form at about  $36r_g$  and below put also constraint on the location of the X-ray source. In the case of a point-like source illuminating the plane most of the reprocessing takes place in a region with a radius about  $\sqrt{3}$  of the source height if the disc extends down to the black hole so this height should be of order of  $25r_g$  or somewhat smaller. This requirement is not satisfied by the stationary model 2.1 as the fitted X-ray source height

in this model covers the range of 35 to  $70r_g$ .

In the case of a model with inner radius cut-off  $R_C$  and the X-ray source placed at the height  $R_C$  (model 2.5) half of the reprocessing takes place below the radius  $\sqrt{7}R_C$  which limits  $R_C$  to values smaller than  $\sim 14r_g$ . This requirement is not satisfied since values as large as  $30r_g$  are reached.

In model 2.4 we assumed that the energy released below the cut-off radius is mostly advected under the horizon. However, the comparison of the observed X-ray luminosity with the available one (see Fig. 4) shows that only  $\sim 50\%$  of the energy should be advected and the remaining  $\sim 50\%$  is necessary to explain the observed direct X-ray emission and the reflected component. Such a considerable irradiation flux modifies the distribution of the effective temperature, contrary to the initial assumption. Therefore the model 2.4, although satisfactory from the point of view of the optical/UV data, either does not produce X-rays (contrary to observations) or is not self-consistent (influence of X-rays cannot be neglected).

Model 2.8 is therefore the only disc model (for a mass of the black hole equal  $6 \times 10^7 M_\odot$ ) fully in agreement with the available observations. The other acceptable description of the optical/UV data gives the free-free model (model 2.9); in this case the constraints from the X-ray observations are difficult to apply as it would require the inclusion of additional parameters into the model representing the geometry of the cloud distribution.

#### 4.3 Dependence on global parameters

We explored the dependence on global parameters by fitting models for a few values of the global parameters involved.

The dependence of the results on the assumed mass of the central black hole is essential in all non-stationary disc models. Since we explicitly limited the accretion rate to remain below the Eddington value all non-stationary models give unacceptable fits if the mass of the black hole is  $1 \times 10^7 M_\odot$ . If the black hole is very massive ( $5 \times 10^8 M_\odot$ ) the temperature of the disc becomes too low to account for the far UV emission although models tend to settle themselves onto the solutions without effective cut-off (i.e.  $R_C = 3r_g$ ) in order to ease this problem.

The value of the mass of the black hole about  $1 \times 10^8 M_\odot$  are optimal for all non-stationary models, independent on geometry. The values of  $\chi^2$  for all models are smaller or comparable to the values obtained for  $6 \times 10^7 M_\odot$ ; even models 2.3 and 2.7 are acceptable. What is more, the models ruled out on the basis of having too extended reprocessing region (models 2.1 and 2.5) are perfectly consistent with X-ray data as the cut-off radius decreases with an increase of the mass of the black hole. Also the X-ray bolometric luminosity is smaller and the predicted values agree within  $\sim 50\%$  (apart from model 2.7, as before) with expected values (see Section 4.2). This trend is related to the drop of the disc temperature with an increase of the mass of the central black hole and no need for a large cut-off radius in order to explain the observed low temperature of the thermal emission. However, it is interesting to note that again the best model is model 2.8, this time purely on the basis of having the lowest reduced  $\chi^2$ .

As the stationary models have an energy source of unspecified nature we did not introduce any apriori constraint

on the luminosity. As a result, most models fit the data for all values of the mass of the central black hole. They depend very weakly on the accretion rate of an underlying accretion disc as the X-ray luminosity strongly dominates disc luminosity. Models for low value of the mass of the black hole marginally satisfy the constraints imposed by the total X-ray luminosity (the brightest models exceed the estimated limit only by 40%). Models for high mass are too bright by a factor up to 4. Therefore again the central mass at about  $6 \times 10^7 M_\odot$  is strongly favoured.

The dependence of stationary models on the adopted value of the accretion rate of the disc is very weak as the X-ray luminosity strongly dominates and the contribution of the radiation flux due to the disc viscosity is negligible in comparison with the thermalized X-ray flux.

#### 4.4 Properties of the best models

Constraints from the IUE observational campaign and from the available X-ray data reduced the acceptable models of the nucleus of the Seyfert galaxy NGC 5548 to just two models: non-stationary accretion disc with a corona (model 2.8) and free-free emitting clouds (model 2.9). We cannot favour any of the two models as they are less specific than other models as for the geometry and no additional constraints are available for them.

Both models fit the optical/UV data well as the actual spectra predicted by the models in this frequency band are almost identical. We can see it in Fig. 5 which shows the plot of the two model spectra in one of the highest luminosity states (date 7622) and one of the lowest states (date 7738). The high state spectrum is almost a power law while the low state has significant curvature (actually, it shows a maximum in  $\nu F_\nu$  diagram). Both models follow these changes very well. Both models in low state are somewhat underluminous at 2670 Å which probably indicates systematic error in the subtraction of the BLR contribution.

Some of the properties of the model 2.8 are shown in Fig. 4. The accretion rate (measured in the Eddington units) vary between 0.05 and 0.14. The cut-off radius varies between  $6r_g$  and  $13r_g$  and it is clearly anticorrelated with the X-ray bolometric luminosity. It means that the strength of the corona decreases with increasing accretion rate. Such a trend is in agreement with a period of even stronger UV brightening (Clavel et al. 1992); anticorrelation of cut-off radius with accretion rate may eventually lead to saturation or even a decrease of the available X-ray flux when cut-off radius approaches  $3r_g$  (see Fig. 6).

## 5 DISCUSSION

As it was already concluded in the first paper on the monitoring campaign of the Seyfert galaxy NGC 5548 (Clavel et al. 1991) the optical/UV emission is dominated most of the time by the reprocessing of the X-ray radiation and further observations confirmed this conclusion. Our models also support this trend.

The analysis presented in this paper favours one among the disc-type models of the nucleus: disc/corona model.

We found also the cloud model to be acceptable and at present we are unable to differentiate between them. The comparison is however unfair since acceptable disc models

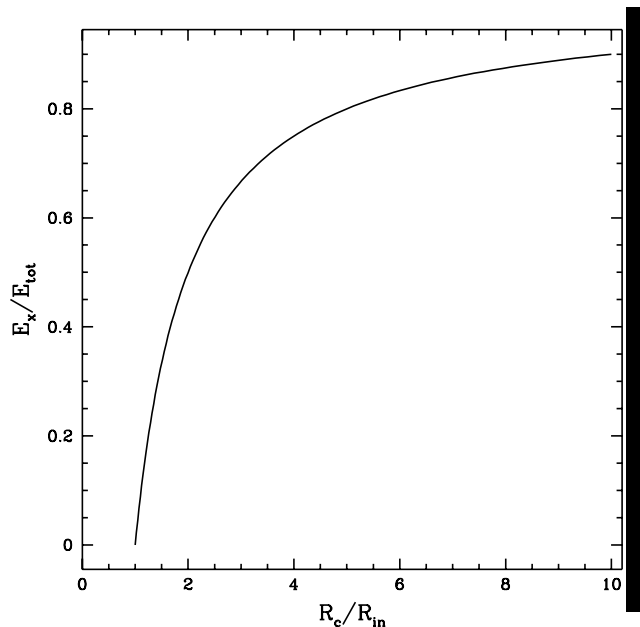


**Figure 6.** Fraction of gravitational energy available for the X-ray emission as a function of the cut-off radius measured in units of the radius of the marginally stable orbit equal  $3r_g$ .

had to satisfy several very strong constraints based by X-ray data whilst optically thin clouds were introduced as purely parametric model without reliable description of their spectra and without a global scenario which would allow to use X-ray constraints to this model as well.

The disk/corona model depends on additional global parameters, including the mass of the central black hole. We adopted the value of  $6 \times 10^7 M_\odot$  (for arguments, see Section 4.1). Lower  $\chi^2$  values for all models, including disc/corona model, were obtained for somewhat larger value ( $1 \times 10^8 M_\odot$ ). However, an attempt to derive the value of the mass of the black hole directly from fits will return this value with a large error.

Other disc type models were ruled out by the fact that models had to satisfy two opposite requirements: (i) the emission region had to have low temperature in order to explain the roll-over of the spectrum in UV band when the object is faint; for a fixed mass, it was achieved by an appropriately large cut-off radius, (ii) the X-ray reflection component has to form close to the black hole so the cut-off radius has to be small enough to allow the disc to be present close to the black hole. As the disc temperature for a given value of the gravitational radius drops with an increase of the mass of the black hole those conflicting requirements are easy to satisfy when the black hole is more massive. In any case the disc emission, particularly when the nucleus is faint, does not extend far into EUV spectral region and is not expected to be seen in soft X-rays.

As the disc/corona model is non-stationary, it poses a question whether any changes of the accretion rate are possible in such a short timescale. In order to estimate that we have to realize that the change in the accretion rate at the innermost part of the disc does not require the actual redistribution of the mass in the disc but it may happen in a thermal timescale, as a transition from one state to another. As the estimates of the timescales of disc/corona system are

not available we may use just the thermal timescales of the standard disc based on the viscosity as described by Shakura & Sunyaev (1973). These timescales, as functions of the wavelength, were carefully estimated by Siemiginowska & Czerny (1989). Assuming the luminosity to the Eddington luminosity ratio as derived from the model (i.e. 0.05 - 0.14) and the observed range of the  $F_\lambda$  at 1350 Å we obtain the timescales below 1 day for the viscosity parameter  $\alpha$  equal 0.1 which is well within the required limits.

The second model representing the optically thin clouds is also acceptable. Unfortunately it is not specific enough in its present form to allow any tests based on the properties of X-ray emission. This model may also have difficulties to account for the temporary brightening in UV or in soft X-rays which were sometimes observed when the source was bright (but not during the campaign analysed in this paper). To account for such a phenomenon it would be necessary to allow for some viscous dissipation within clouds. However, no specific models of such a clumpy disc are available at present.

The similarity of the two model spectra when fitted to the optical/UV data clearly shows that it is very difficult to differentiate between the two models. Careful reduction of the data, removal of the starlight and the BLR contribution are essential but not enough to favour any of the two possibilities, and actually even more models are acceptable if the mass of the central black hole is allowed to be somewhat higher.

Therefore, the problem lies clearly in too small dynamical range of the studied spectra. However, the solution of the problem is not easy.

It is relatively simple to include an additional point at  $\sim 8000$  Å, as the entire spectra are in principle available although their reduction is by no means simple.

Extension of the monitoring from optical to soft X-ray band would in principle help significantly but it would make the problem of modelling very complex. Both optically thin clouds and disc/corona model spectra cannot be represented by simple models considered in this paper (see Collin-Souffrin et al. 1996 for clouds and Źycki et al. 1994 for disc reprocessing). Reliable models are not available yet for the soft X-ray band. However, as soon as acceptable models are proposed such broader fits may be strongly constraining.

More direct use can be made from hard X-ray band monitoring if the data is accurate enough to show the variations in the reflected component. The comparison with such a data would not necessarily require much more sophisticated models than currently described. Particularly interesting data would be collected when the source is rather faint since such observations might determine whether the innermost part of the disc actually undergoes a structural change or whether accretion rate is temporarily reduced. However, such monitoring is beyond the present possibilities.

## 6 CONCLUSIONS

On the basis of the analysis of the IUE observational campaign of the Seyfert galaxy NGC 5548 and the constraints from the X-ray observations we show that the nuclear emission can be fitted by a model of a non-stationary accretion

disc with a corona. Simple analytic free-free formula representing the emission of a distribution of clouds optically thin for absorption gives an acceptable description of the optical/UV data alone. There is no possibility to distinguish between these two models on the basis of the present data as it is not clear how to imply the constraints from the X-ray data in the case of cloud model. Any further progress can be only made if the research is extended either towards careful studies, both observational and theoretical, of the spectral features like emission lines and edges, or towards broadening of the spectral range towards soft X-rays and/or hard X-rays.

## ACKNOWLEDGMENTS

We would like to thank Chris Done, the referee, for extremely helpful remarks which lead to clarification of the line of argument. We are grateful to Andrzej Sołtan for very helpful discussions of the statistical problems, to Asia Kuraszkiewicz for the discussions of the starlight subtraction and to Aneta Siemiginowska for her subroutine to compute the Gaunt factor. This project was partially supported by grants no. 2P30401004 and no. 2P03D00410 of the Polish State Committee for Scientific Research. This research has made use of the NASA/IPAC Extragalactic Database (NED) operated by the Jet Propulsion Laboratory, Caltech.

## REFERENCES

- Antonucci, R.R.J., Barvainis, R., 1988, ApJ, 332, L13
- Barvainis, R., 1993, ApJ, 412, 513
- Clavel, J. et al., 1991, ApJ, 366, 64
- Clavel, J. et al. 1992, ApJ, 393, 113
- Collin-Souffrin, S., 1991, A&A, 249, 344
- Collin-Souffrin, S., Czerny, B., Dumont, A.-M., Źycki, P.T., 1996, A & A (in press)
- Done, C., Krolik, J.H., 1996, ApJ (in press)
- Done, C., Pounds, K.A., Nandra, K., Fabian, A.C., 1995, MNRAS, 275, 417
- Ferland, G., Korista, K.T., Peterson, B.M., 1990, ApJ, 363, L21
- Gronenschild, E.H.B.M., Mewe, R., 1978, A&A Suppl. Ser., 32, 283
- Guilbert, P.W., Rees, M., 1988, MNRAS, 233, 475
- Henri, G., Pelletier, G., 1991, ApJ, 383, L7
- Kotilainen, J.K., Ward, M.J., 1994, MNRAS, 266, 953
- Krolik, J.H., Horne, K., Kallman, T.R., Malkan, M.A., Edelson, R.A., Kriss, G.A., 1991, ApJ, 371, 541
- Krolik, J.H., Kriss, G.A., 1995, ApJ, 447, 512
- Kusunose, M., Zdziarski, A.A., 1994, ApJ, 422, 737
- Liang, E.P., Li, H., 1995, A&A, 298, L45
- Liang, E.P., Price, R.H., 1977, ApJ, 218, 247
- Lightman, A.P., White, T.R., 1988, ApJ, 335, 57
- Loska, Z., Czerny, B., Szczerba, R., 1993, MNRAS, 262, L31
- Loska, Z., Czerny, B., 1990, MNRAS, 244, 43
- Malkan, M.A., 1991, in Structure and Properties of Accretion Disks, ed. C. Bertout et al., Paris, Editions Frontiers, p. 165
- Maoz, D., et al., 1993, ApJ., 404, 576
- Marshall, H.L., Fruscione, A., Carone, T.E., 1995, ApJ, 439, 90
- Mushotzky, R.F., Fabian, A.C., Iwasawa, K., Kunieda, H., Matsuo, M., Nandra, K., Tanaka, Y., 1995, MNRAS, 272, L9
- Nandra, K. et al. 1991, MNRAS, 248, 760
- Nandra, K. et al. 1993, MNRAS, 260, 504
- Nandra, K., Pounds, K.A., 1994, MNRAS, 268, 405

Narayan, R., Yi, I., 1995, *ApJ*, 444, 231  
 Paczyński, B., 1978, *Acta Astron.*, 28, 241  
 Peterson, B.M., et al. 1991, *ApJ*, 368, 119  
 Peterson, B.M. et al. 1992, *ApJ*, 392, 470  
 Peterson, B.M., et al. 1994, *ApJ*, 425, 622  
 Press, W.H., Flannery, B.P., Teukolsky, S.A., Wetterling, W.T.,  
     1989, *Numerical Recipes in Pascal: The Art of Scientific  
         Computing*, Cambridge University Press, New York  
 Rokaki, E., Collin-Souffrin, S., Magnan, C., 1993, *A&A*, 272, 8  
 Romanishin, W., et al. 1995, *ApJ*, 455, 516  
 Ross, R.R., Fabian, A.C., 1993, *MNRAS*, 261, 74  
 Shakura, N.I., Sunyaev, R.A., 1973, *A&A*, 24, 337  
 Shapiro, S.L., Lightman, A.P., Eardley, D.M., 1976, *ApJ*, 204,  
     187  
 Siemiginowska, A., Czerny, B., 1989, *MNRAS*, 239, 289  
 Sivron, R., Tsuruta, S., 1993, *ApJ*, 402, 420  
 Wamsteker, W., et al., 1990, *ApJ*, 354, 446  
 Wandel, A., Liang, E.P., 1991, *ApJ*, 283, 842  
 Wanders, I. et al., 1995, *ApJ*, Nov.10  
 Ward, M., Elvis, M., Fabbiano, G., Carleton, N.P., Willner,  
     S.P., Lawrence, A., 1987, *ApJ*, 315, 74  
 Źycki, P.T., Collin-Souffrin, S., Czerny, B., 1995, *MNRAS*, 277,  
     70  
 Źycki, P.T., Czerny, B., 1994, *MNRAS*, 266, 653  
 Źycki, P.T., Krolik, J.H., Zdziarski, A.A., Kallman, T., 1994,  
     ApJ, 437, 597

This paper has been produced using the Blackwell Scientific  
 Publications TeX macros.